



Numerical study on mixing performance of 3D passive micromixer with scaling elements

Jiajia Xu¹ · Xueye Chen¹

Received: 4 April 2019 / Accepted: 14 September 2019 / Published online: 23 September 2019
© The Brazilian Society of Mechanical Sciences and Engineering 2019

Abstract

In this study, we applied scaling elements to design micromixers. We designed four passive micromixers with different structures, including common micromixer, common micromixer with scaling elements, snake-like micromixer, and snake-like micromixer with scaling elements (SMWSE). We used COMSOL Multiphysics 5.2a software to simulate and analyze. The numerical simulation results show that the scaling elements can cause the chaotic convection between the fluids with different concentrations. Through the analysis of the variation in concentration and velocity on the cross section of micromixers, it can conclude that the micromixer with scaling elements has high mixing efficiency, and the mixing efficiency of SMWSE is more than 92% at all fluid velocities.

Keywords Mixing efficiency · Scaling elements · Chaotic convection

1 Introduction

Microfluidic systems have a good application prospect in chemical analysis and biological engineering and other fields. Mixing process is fundamental and important in chemical analysis [1–3]. However, in most cases, the fluid is in laminar flow and the mixing mechanism is diffusion [4, 5]. As an important part of microfluidic chip, micromixer plays an important role in improving the mixing efficiency in chemical analysis. Micromixers can be divided into passive micromixers and active micromixers according to the causes of fluid mixing [6]. The active micromixers can disturb the flow of fluids in microchannel through the external energy fields, which accelerates the fluid diffusion and convection, and improved the mixing efficiency. The common external energy fields include electric field, magnetic field, and ultrasonic [7, 8]. The requirements for mixing time and microchannel length of active micromixers are lower than those of passive micromixers. However, active micromixers are usually multilayer structures and not easy to make. The

passive micromixers mainly rely on changing the internal structures to change the flow trajectory of fluids and improve the mixing efficiency. The main principle of passive micromixers to improve the mixing efficiency is to enhance the molecular diffusion and the chaotic convection.

The passive micromixer improves the mixing efficiency mainly by changing the design of geometric structures. Passive micromixers can be divided into two types of mixing mechanisms, namely chaotic convection and lamination [9–13]. In this study, we designed 3D passive micromixers and improved the mixing efficiency by generating chaotic convection in micromixers. Niu and Lee [14] designed a chaotic micromixer with multiple side microchannels; it can stir the fluid through the side microchannels. Mouza et al. [15] designed a novel micromixer by combining the structure of curved channel; this chaotic micromixer has better mixing performance than planar meandering micromixer at a lower Dean number. Liu designed a three-dimensional micromixer with a “c-shaped” repeating element, which uses chaotic convection to enhance fluid mixing. They used wet-etching technology on silicon chips to achieve a three-dimensional geometry [16]. Chen et al. had done a lot of simulation and numerical researches, which prove that the numerical simulation based on hydrodynamics is reliable for studying the performance of micromixers [17–24]. Lee et al. did numerical simulations of six different shapes of micromixers. The optimized micromixer has higher mixing efficiency and

Technical Editor: Daniel Onofre de Almeida Cruz, D.Sc.

✉ Xueye Chen
xueye_chen@126.com

¹ Faculty of Mechanical Engineer and Automation, Liaoning University of Technology, Jinzhou 121001, China

lower pressure drop [25]. Su et al. [26] studied the fluid mixing in the curved microchannels and found that the mixing efficiency was proportional to the diffusion rate and density ratio, and inversely proportional to the microchannel width and flow velocity. The micromixer designed in this paper is composed of microchannels with right angles, and scaling structures are placed in the middle of the microchannel to improve the mixing efficiency. The optimal structure has a high mixing efficiency of more than 93% within the range of Re 0.04–22.

In this study, we designed four kinds of three-dimensional passive micromixers with different structures, including CM, CMWSE, SM, and SMWSE. The chaotic convection occurred in the microchannel and the mixing efficiency is improved. In the discussion section, we analyzed the variation in cross section concentration and mixing efficiency curves of micromixers. The simulation results show that the micromixer with scaling structure has higher mixing efficiency. The SMWSE has the characteristics of high mixing efficiency at all fluid velocities.

2 Micromixer designs

Figure 1 shows the schematic diagram of the four passive micromixers. The fluids flow in from the two inlets on the left side and flow out from the right outlets. The total length of the micromixer is $17\ \mu\text{m}$, and the height of the microchannel is $1\ \mu\text{m}$. Figure 1a shows the structure of common micromixer (CM). Figure 1b shows the structure of common micromixer with scaling element (CMWSE); p is a scaling element. Figure 1c shows the structure of snake-like micromixer (SM). Figure 1d shows the structure of snake-like micromixer with scaling element (SMWSE).

3 Theoretical background

3.1 Governing equations

The Navier–Stokes equation is usually used to describe the dynamic characteristics of the fluid velocity and the pressure of incompressible fluid flow. It can be expressed as follows:

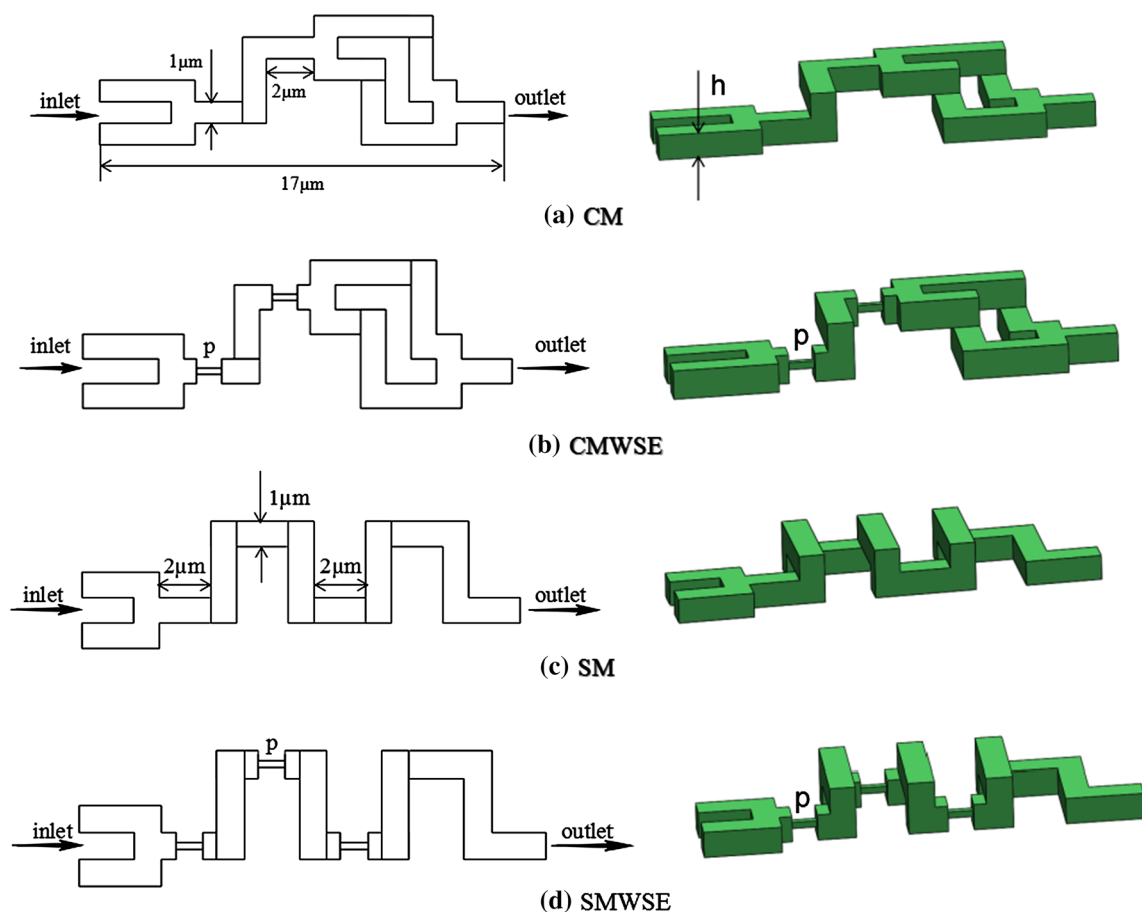


Fig. 1 The structure of the four passive micromixers ($h = 1\ \mu\text{m}$, $p = 1\ \mu\text{m} \times 0.25\ \mu\text{m} \times 0.25\ \mu\text{m}$)

$$\rho \frac{\partial u}{\partial t} + \rho(u \cdot \nabla)u + \nabla p - \eta \nabla^2 u = 0 \tag{1}$$

$$\nabla \cdot u = 0 \tag{2}$$

where u is velocity vector, ρ is the fluid density, t is the time, η is the dynamic viscosity and p is the pressure. Convection–diffusion equation can be applied to describe the mixing efficiency of different concentrations of reagents, as follows:

$$\frac{\partial c}{\partial t} + \nabla \cdot (-D \nabla c) = -u \cdot \nabla c \tag{3}$$

where c is the species concentration and D is the diffusion coefficient.

Calculating the mixing efficiency gives us a more intuitive understanding of the mixing performance of fluids. The calculation equation of mixing efficiency is as follows:

$$M = 1 - \sqrt{\frac{1}{N} \sum_{i=1}^N \left(\frac{c_i - \bar{c}}{\bar{c}} \right)^2} \tag{4}$$

where N is the total number of sampling points, c_i is the standard concentration and \bar{c} is the expected standard concentration, respectively. Mixing efficiency ranges from 0 (0%, not mixing) to 1 (100%, full mixed).

Reynolds number (Re) is an important parameter for studying the mixing efficiency of fluids, which is defined as:

$$Re = \frac{\rho D_h U}{\eta} \tag{5}$$

where ρ is the fluid density, D_h is the hydraulic diameter of the cross section of the microchannel, $D_h = 1 \mu\text{m}$, U is the average velocity of the fluid and η is the dynamic viscosity of fluid.

3.2 Simulation setting

In this study, COMSOL Multiphysics 5.2a is used to conduct numerical simulation on the four kinds of passive micromixers which designed with different structures. Micromixer at the inlets is speed, and the boundary condition at the outlet is pressure. The fluid channel wall is set to compressible and no-slip boundary conditions. The material selected for the study is liquid water, whose dynamic viscosity is $V = 1 \times 10^{-6} \text{ m}^2/\text{s}$ and the diffusion constant $D = 1.1 \times 10^{-10} \text{ m}^2/\text{s}$. The initial concentration conditions of the fluids are, respectively, set to be $C_1 = 1 \text{ mol/L}$ and $C_2 = 0 \text{ mol/L}$.

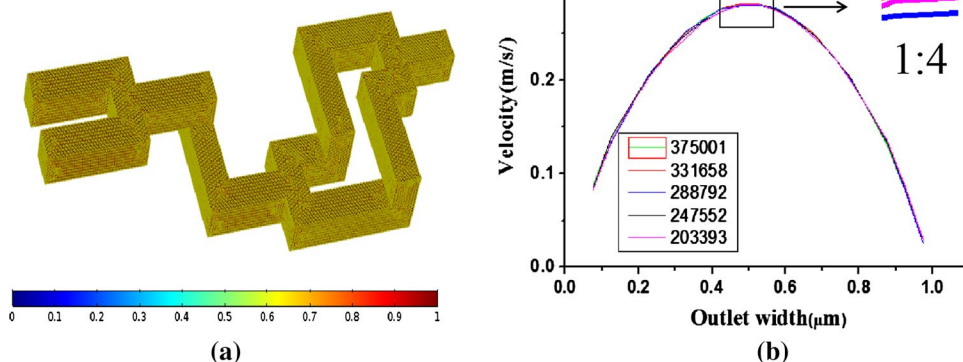
It is important to choose a reasonable grid system. A good grid system selection can improve the accuracy of simulation results and reduce the computing time. In this study, we choose the free mesh of triangle to divide geometry; the element growth rate is 1.1. Figure 2a shows the grid system of CM; the color legend represents the quality of elements. The CM has 331,685 elements. The minimum element quality is 0.0139. Figure 2b shows the local velocity profiles at the outlet of CM at $V = 0.1 \text{ m/s}$ with four mesh refinements. The 331,658 grid numbers corresponding to the green curve are the best result to obtain a mesh-independent solution. Other designs in the paper are divided according to the results of the grid independency test. The computational time required for simulation of a micromixer at one velocity is 268 s. The simulation results are correct and reliable according to FEM theory.

4 Results and discussion

4.1 The analysis of mixing performance on CM

Figure 3 shows the simulation result of CM. For the convenience of the following discussion, sections a, b, and c are the objects of discussion.

Fig. 2 **a** The grid system of CM with 331, 685 elements and **b** the velocity profiles along the middle line at the outlet at $V = 0.1 \text{ m/s}$ (color figure online)



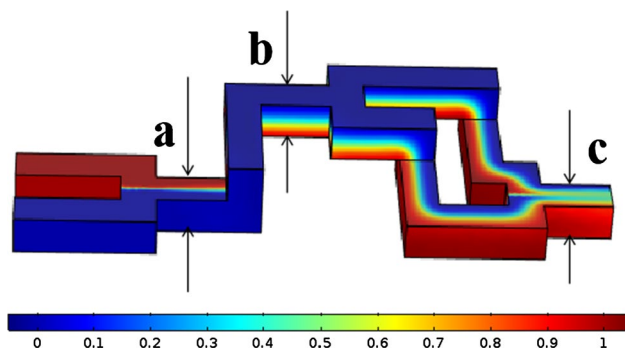


Fig. 3 The mixing performance of CM at $Re = 1$

Figure 4 shows the concentration changes on the cross section of CM at different Re . The mixing performance of the same cross section is different with the changes in Re according to the simulation results. The more uniform the color of the cross section concentration, the higher the mixing efficiency of fluids. Figure 5 shows the mixing efficiency of CM under different Re . From the mixing efficiency curve of CM, we can conclude that the mixing efficiency decreases first and then increases. When Re is 1, the mixing efficiency is the lowest. When Re is 0.04, the mixing form is dominated by molecular diffusion due to the low velocity. The molecular diffusion time is long, and thus the mixing efficiency is high in this time. When Re is within the range of 0.04–1, the time required for molecular diffusion is shortened although the flow velocity is increased, and thus the mixing efficiency is not improved. When Re is within the range of 1–20, the mixing efficiency increases gradually with the increase in Re . The reason for this phenomenon

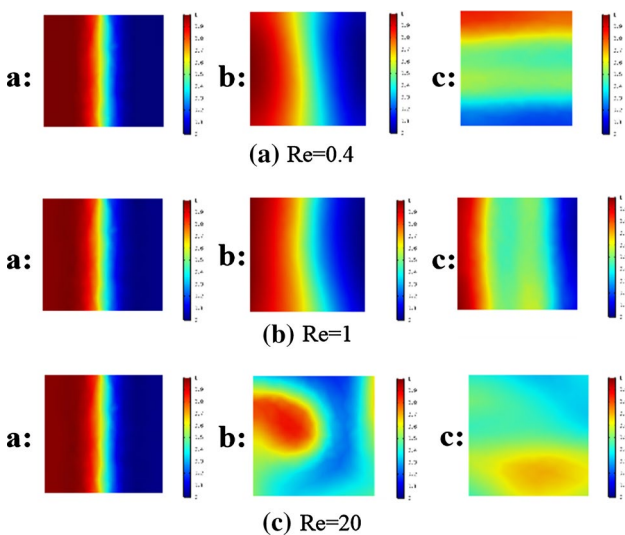


Fig. 4 The concentration changes on cross sections of CM at different Re (color figure online)

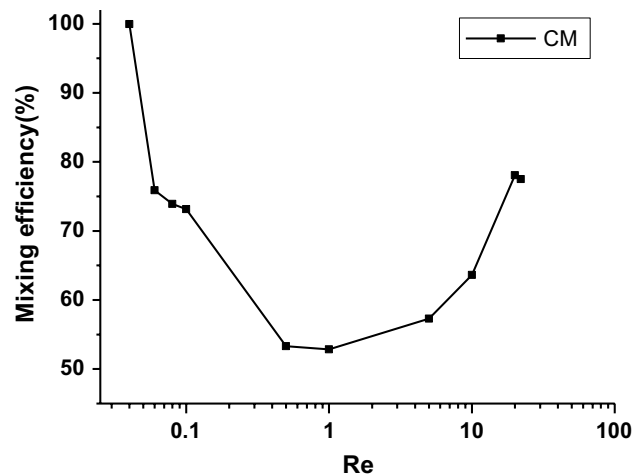


Fig. 5 The mixing efficiency of CM

is that chaotic convection occurs when the fluid velocity increases, which improves the mixing efficiency.

Figure 6 shows the fluid velocity distribution on the cross section of CM. The arrows on the cross section represent the flow direction. It can be clearly seen from the simulation results that the direction of the fluid is almost uniform and no chaotic convection occurs when $Re = 1$, and thus the mixing efficiency is low. When $Re = 20$, the chaotic convection occurs in the microchannel of the micromixer, which improves the mixing areas and time, and thus the mixing efficiency is improved.

4.2 The analysis of mixing performance on CMWSE

In order to further improve the mixing efficiency, we added two scaling elements based on CM structure to form the CMWSE. Figure 7 shows the concentration results of CMWSE, a, b, and c are where the concentration cross section is. As the results show, when $Re = 1$, the mixing performance of CMWSE is better than CM.

Figure 8 shows the mixing efficiency of CMWSE under different Re . When Re is in the range from 0.04 to 5, it can be concluded that the mixing efficiency gradually decreases with the increase in Re . When $Re = 5$, the mixing efficiency of CMWSE reaches a minimum of 80%. When the Re increases gradually in the range of 5–22, the mixing efficiency of the micromixer increases gradually. The mixing efficiency finally reaches 97% and tends to be stable.

Figure 9 shows the velocity changes on cross section of CMWSE, the position of cross section a, b, c, as shown in Fig. 7. The simulation results show that when $Re = 1$, the fluid is in laminar flow and the velocity direction of the fluid is approximately the same. There is no obvious chaotic convection in microchannel. When $Re = 20$, the chaotic convection occurs in cross section c. By comparison, it is found that

Fig. 6 The fluid velocity variation on cross sections of CM

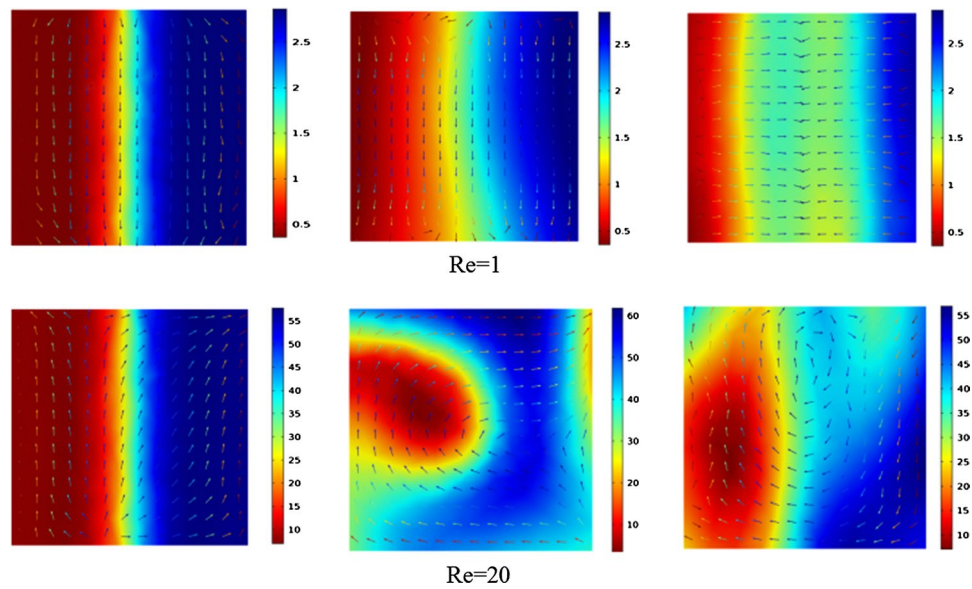
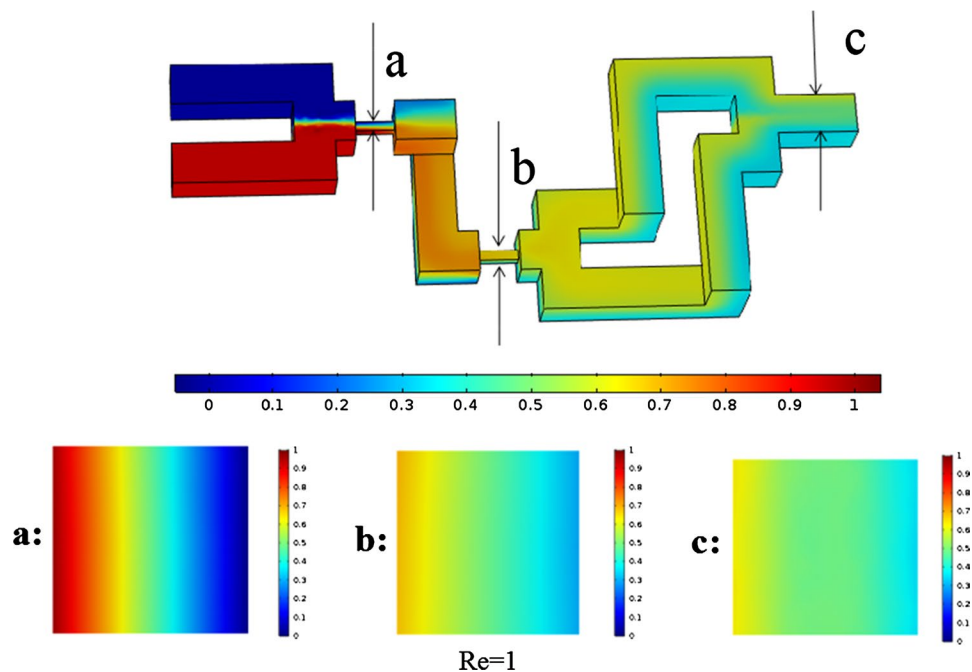


Fig. 7 The mixing performance of CMWSE at $Re = 1$



the more obvious of the chaotic convection phenomenon, the higher of the mixing efficiency. The results show that the chaotic convection can improve the mixing efficiency of the micromixer.

4.3 The analysis of mixing performance on SM

Figure 10 shows the mixing efficiency of SM under different Re . As the results show, when Re is in the range of 0.04–1, it can be concluded that the mixing efficiency gradually decreases with the increase in Re . When $Re = 1$,

the mixing efficiency reaches the lowest of 60%. According to the above discussion, it can be concluded that the mixing efficiency is related to the existence of chaotic convection in the microchannel. There is no obvious chaotic convection phenomenon in the micromixer when $Re = 1$, and thus the mixing efficiency is the lowest. The mixing performance of SM is shown in Fig. 11. When Re increases gradually in the range of 1–22, the mixing efficiency of the micromixer increases gradually and reaches 92% when the $Re = 22$.

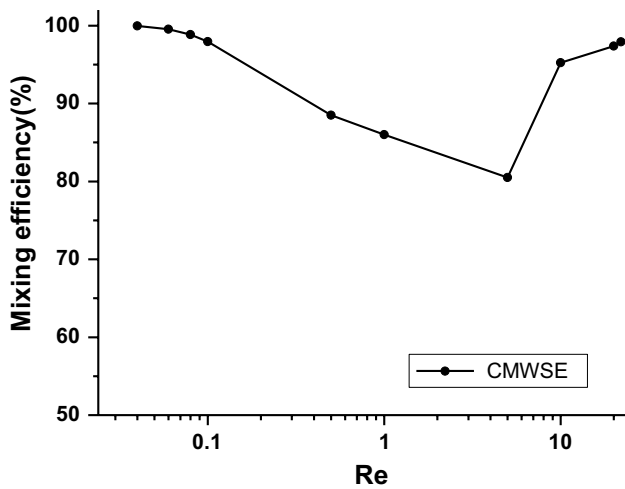


Fig. 8 The mixing efficiency of CMWSE

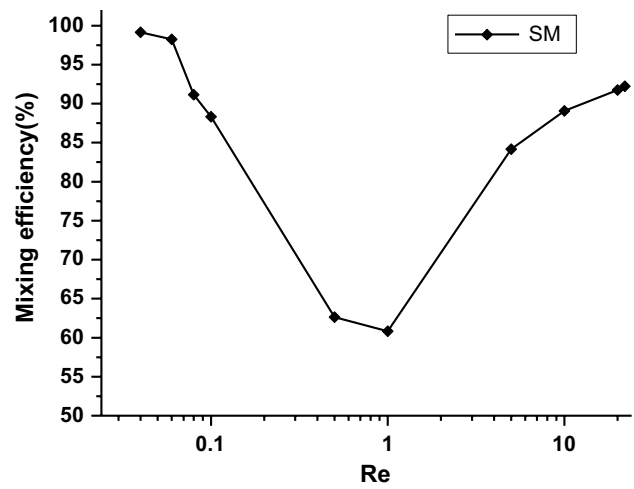


Fig. 10 The mixing efficiency of SM

4.4 The analysis of mixing performance on SMWSE

We added scaling elements based on SM structure to form the SMWSE. The SMWSE has three scaling elements, and the simulation results are shown in Fig. 12. When $Re = 1$, the mixing performance of SMWSE is better than SM. Figure 13 shows the mixing efficiency of SMWSE. As the results show, when Re is in the range of 0.04–0.1, the mixing form is dominant by molecular diffusion, and thus the mixing efficiency can reach above 99%. When Re is within the range of 0.1–1, the mixing efficiency of the fluid decreases with the increase in the flow velocities. At this time, the molecular diffusion time is shortened, and the chaotic convection phenomenon in the microchannel is not obvious, and thus the mixing efficiency is reduced. When $Re = 1$, the mixing efficiency of SMWSE is above 92%, which indicates that SMWSE has a good mixing performance. When Re is

in the range of 1–22, the chaotic convection phenomenon is gradually obvious in the microchannel, and thus the mixing efficiency is improved. Figure 14 shows the chaotic convection phenomenon in the micromixer at $Re = 20$. The above results show that the mixing efficiency of the micromixer with scaling elements is higher. The scaling elements can improve the mixing efficiency by generating the chaotic convection phenomenon in the micromixer.

4.5 The pressure drop and mixing efficiency of the four passive micromixers

Besides the mixing efficiency, the pressure drop is another important parameter to analyze the mixing performance of passive micromixers. A stable pressure drop variation ensures that the micromixer is not crushed during fabrication. Figure 15 shows the simulation results of CM, CMWSE, SM, and SMWSE on pressure drop. We measured

Fig. 9 The fluid velocity changes on cross section of CMWSE

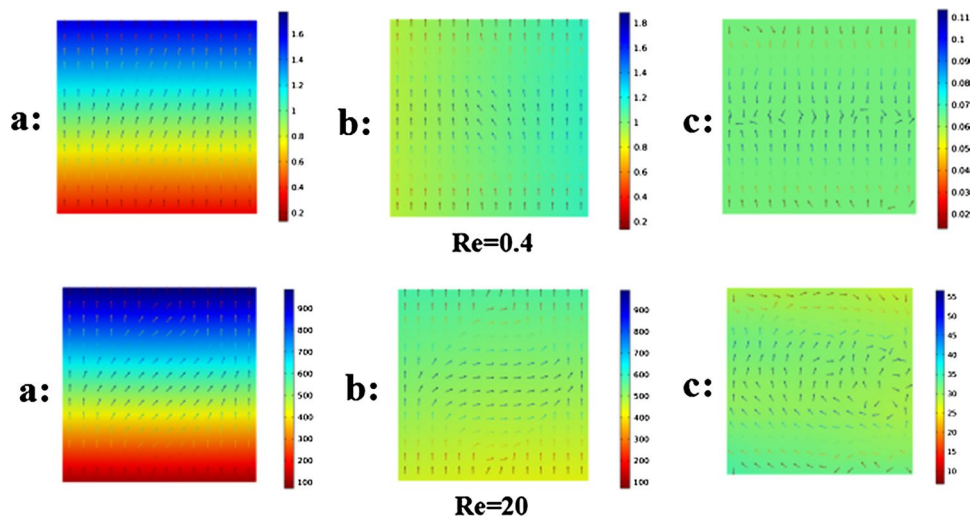


Fig. 11 The concentration change in SM on cross section at $Re = 1$

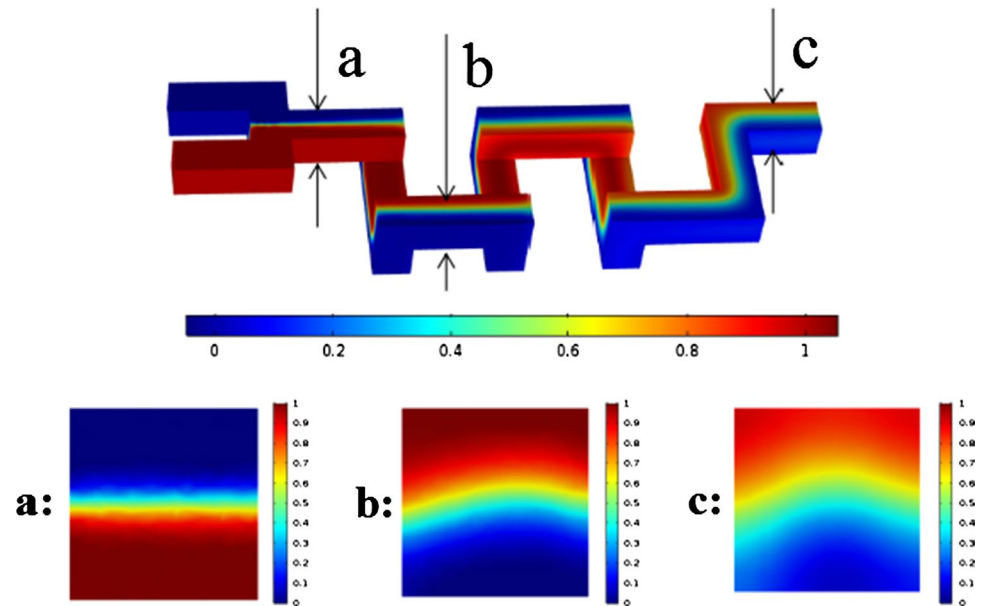
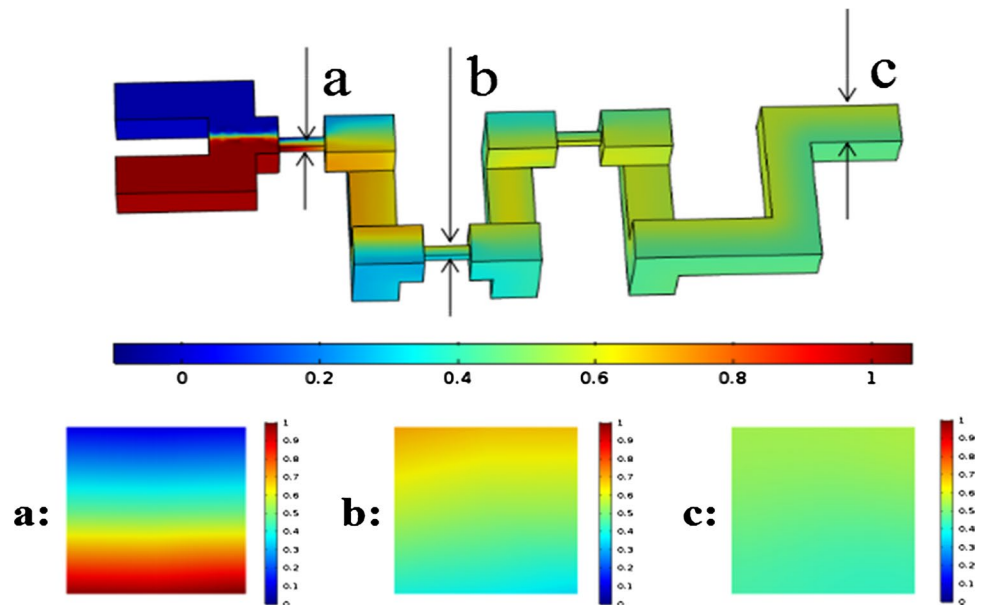


Fig. 12 The mixing performance of SMWSE at $Re = 1$



the pressure drop of the micromixer at $Re = 0.04, 0.06, 0.08, 0.1, 0.5, 1, 5, 10, 20$. The pressure drop increases with Re in all micromixers. As the results show, the micromixer with scaling elements has the higher pressure drop than the micromixer with no scaling elements. From the above discussion, SMWSE has the highest mixing efficiency, but at the same time its pressure drop is also the highest.

The mixing efficiency curves of four passive micromixers under different Re are shown in Fig. 16. As the results show, the SMWSE has the highest mixing efficiency at all velocities. The minimum mixing efficiency of SMWSE is 92% at $Re = 1$. The CM has the lowest mixing efficiency at all velocities.

5 Conclusion

In this paper, we designed four passive micromixers with different structures. The mixing efficiency, pressure drop, and fluid flow in the microchannel were analyzed. The simulation results show that the order of mixing efficiency of micromixers from low to high is CM, CMWAE, SM, and SMWSE. The variation characteristics of mixing efficiency curves are similar; the mixing efficiency decreases first and then increases with the increase in Re . CM, CMWSE, and SM have the lowest mixing efficiency when $Re = 1$, and when $Re = 5$, SMWSE has the lowest mixing

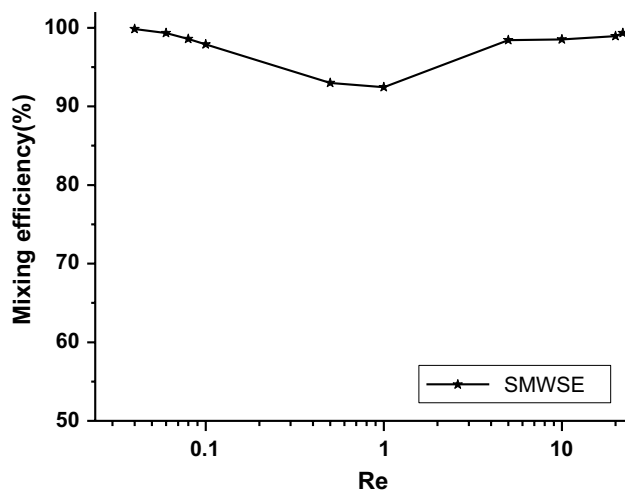


Fig. 13 The mixing efficiency of SMWSE

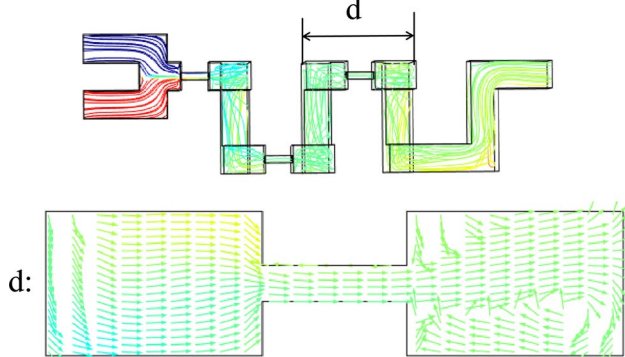


Fig. 14 The fluid flow behavior of SMWSE at $Re = 20$

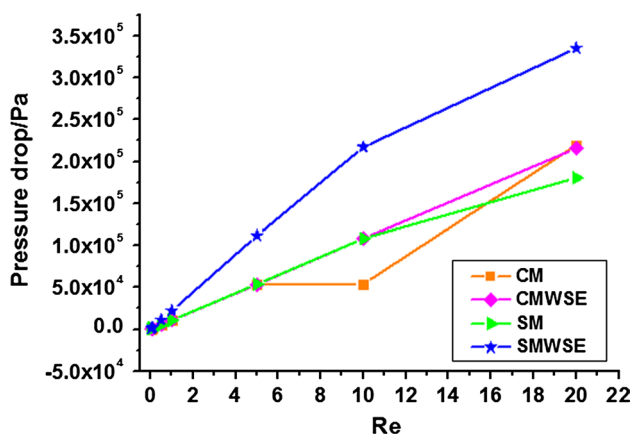


Fig. 15 The pressure drop of four passive micromixers at different Re

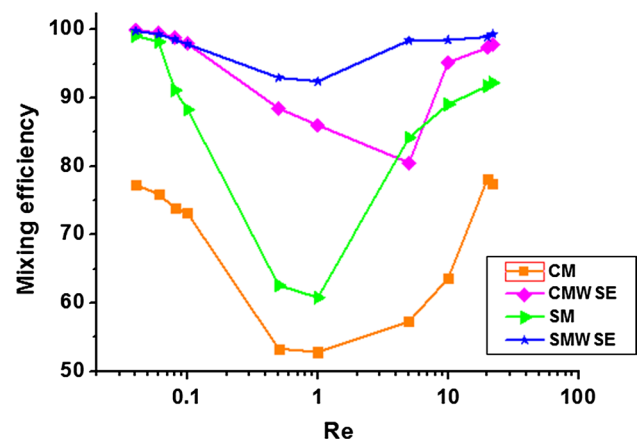


Fig. 16 The mixing efficiency of four passive micromixers at different Re

efficiency. The SMWSE has the highest mixing efficiency of above 92% at all velocities, but at the same time it has the highest pressure drop. The scaling elements can cause the chaotic convection between the fluids with different concentrations and thus improve the mixing efficiency of micromixer. The pressure drop of micromixer with scaling elements is higher than the micromixer with no scaling elements. This structure can be widely used in the microfluidic system and microchemical-reaction devices.

Acknowledgements This work was supported by Liaoning Natural Science Foundation (2019-MS-169), The Key Project of Department of Education of Liaoning Province (JZL201715401), Liaoning Bai-QianWan Talents Program. We sincerely thank Prof. Chong Liu for his kind guidance.

References

1. Fair RB, Khlystov A, Taylor TD et al (2007) Chemical and biological applications of digital-microfluidic devices. *IEEE Des Test Comput* 24(1):10–24
2. Beebe DJ, Mensing GA, Walker GM (2002) Physics and applications of microfluidics in biology. *Annu Rev Biomed Eng* 4(1):261–286
3. Fan X, White IM (2011) Optofluidic microsystems for chemical and biological analysis. *Nat Photonics* 5(10):591
4. Hardt S, Schönfeld F (2003) Laminar mixing in different interdigital micromixers: II. Numerical simulations. *AIChE J* 49(3):578–584
5. Bothe D, Stemich C, Warnecke HJ (2006) Fluid mixing in a T-shaped micro-mixer. *Chem Eng Sci* 61(9):2950–2958
6. Hessel V, Löwe H, Schönfeld F (2005) Micromixers—a review on passive and active mixing principles. *Chem Eng Sci* 60(8–9):2479–2501
7. Lu LH, Ryu KS, Liu C (2002) A magnetic microstirrer and array for microfluidic mixing. *J Microelectromech Syst* 11(5):462–469
8. Ryu KS, Shaikh K, Goluch E et al (2004) Micro magnetic stir-bar mixer integrated with parylene microfluidic channels. *Lab Chip* 4(6):608–613

9. Shih TR, Chung CK (2008) A high-efficiency planar micromixer with convection and diffusion mixing over a wide Reynolds number range. *Microfluidics Nanofluidics* 5(2):175–183
10. Kim DS, Lee SW, Kwon TH et al (2004) A barrier embedded chaotic micromixer. *J Micromech Microeng* 14(6):798
11. Hossain S, Ansari MA, Kim KY (2009) Evaluation of the mixing performance of three passive micromixers. *Chem Eng J* 150(2–3):492–501
12. Chung CK, Shih TR (2008) Effect of geometry on fluid mixing of the rhombic micromixers. *Microfluidics Nanofluidics* 4(5):419–425
13. Xia HM, Wan SYM, Shu C et al (2005) Chaotic micromixers using two-layer crossing channels to exhibit fast mixing at low Reynolds numbers. *Lab Chip* 5(7):748–755
14. Niu X, Lee YK (2003) Efficient spatial-temporal chaotic mixing in microchannels. *J Micromech Microeng* 13(3):454
15. Mouza AA, Patsa CM, Schönfeld F (2008) Mixing performance of a chaotic micro-mixer. *Chem Eng Res Des* 86(10):1128–1134
16. Liu RH, Stremmer MA, Sharp KV et al (2000) Passive mixing in a three-dimensional serpentine microchannel. *J Microelectromech Syst* 9(2):190–197
17. Chen X, Li T et al (2016) A novel design for passive micromixers based on topology optimization method. *Biomed Microdevice* 18(4):1–15
18. Chen X, Li T, Zeng H et al (2016) Numerical and experimental investigation on micromixers with serpentine microchannels. *Int J Heat Mass Transf* 98:131–140
19. Chen X, Liu C, Xu Z et al (2013) An effective PDMS microfluidic chip for chemiluminescence detection of cobalt (II) in water. *Microsyst Technol* 19(1):99–103
20. Chen X, Shen J, Zhou M (2016) Rapid fabrication of a four-layer PMMA-based microfluidic chip using CO₂-laser micromachining and thermal bonding. *J Micromech Microeng* 26(10):107001
21. Chen X, Li T (2017) A novel passive micromixer designed by applying an optimization algorithm to the zigzag microchannel. *Chem Eng J* 313:1406–1414
22. Chen X, Zhang L (2018) Review in manufacturing methods of nanochannels of bio-nanofluidic chips. *Sens Actuators B Chem* 254:648–659
23. Chen X, Zhao Z (2017) Numerical investigation on layout optimization of obstacles in a three-dimensional passive micromixer. *Anal Chim Acta* 964:142–149
24. Chen X, Li T, Shen J et al (2017) From structures, packaging to application: a system-level review for micro direct methanol fuel cell. *Renew Sustain Energy Rev* 80:669–678
25. Lee JI, Kim CK (2018) Performance assessment of passive micromixer using numerical analysis. *J Korea Converg Soc* 9(10):237–242
26. Su T, Cheng K, Wang J et al (2019) A fast design method for passive micromixer with angled bend. *Microsyst Technol*. <https://doi.org/10.1007/s00542-019-04433-z>

Publisher's Note Springer Nature remains neutral with regard to jurisdictional claims in published maps and institutional affiliations.